

**RESEARCH ARTICLE**

# On the changing relationship between North Pacific climate variability and synoptic activity over the Hawaiian Islands

Oliver Elison Timm<sup>1</sup>  | Siyu Li<sup>1,2</sup> | Jiping Liu<sup>1</sup> | David W. Beilman<sup>3</sup> 

<sup>1</sup>Department of Atmospheric and Environmental Sciences, University at Albany, Albany, New York

<sup>2</sup>Department of Environmental and Sustainable Engineering, University at Albany, Albany, New York

<sup>3</sup>Department of Geography & Environment, University of Hawai'i at Mānoa, Honolulu, Hawaii

**Correspondence**

Oliver Elison Timm, Department of Atmospheric and Environmental Sciences, University at Albany, 1400 Washington Avenue – ES 351 Albany, NY.  
Email: oelisontimm@albany.edu

**Funding information**

Climate Program Office, Grant/Award Numbers: NA15OAR4310146, NA15OAR4310163; Division of Atmospheric and Geospace Sciences, Grant/Award Numbers: 1502951, 1502984; U.S. Geological Survey, Grant/Award Number: G18AC00021

**Abstract**

The teleconnection between tropical and extratropical climates in the North Pacific and continental regions of eastern Asia and western North America is known to vary on decadal to multidecadal time scales. In this study, the teleconnection pattern is studied with observational and reanalysis data products. The regional focus is set on the Hawaiian Islands in the central subtropical part of the North Pacific. By analysing correlations between regional climate indices and large-scale climate modes during the years 1980 and 2014, it was found that the correlation between El Niño—Southern Oscillation (ENSO) and the synoptic weather activity over the Hawaiian Islands decreased over time. Composite analysis of the geopotential height anomalies and upper level winds suggest that the systematic shift in the North Pacific Jet (NPJ) position had an impact on the teleconnection between tropical Pacific SST and winter storm activity and precipitation variability in Hawai'i. The change in the correlations and in the NPJ structure coincides with a transition from the positive phase of the Pacific Decadal Oscillation (PDO) towards a neutral and weak negative state. This observation-based study provides a central subtropical Pacific viewpoint in support of the growing body of research studies that have reported a major shift in the Pacific climate system during the mid-1990s. The article further discusses the potential role of decadal-scale changes in the North Pacific Oscillation (NPO) phase in changing the strength of the ENSO teleconnection with synoptic activity over the Hawaiian Islands. The results of this study are relevant to paleoclimate interpretation of individual proxy records as well as for regional downscaling of future rainfall for the Hawaiian Islands.

**KEYWORDS**

climate, decadal, Hawai'i, Kona low, rainfall, synoptic, teleconnection

This is an open access article under the terms of the Creative Commons Attribution-NonCommercial-NoDerivs License, which permits use and distribution in any medium, provided the original work is properly cited, the use is non-commercial and no modifications or adaptations are made.

© 2020 The Authors *International Journal of Climatology* published by John Wiley & Sons Ltd on behalf of Royal Meteorological Society.

## 1 | INTRODUCTION

The subtropical North Pacific climate zone is located between the equatorial tropical climate zone and the mid-latitude storm tracks to the north. This transition zone between tropical and extratropical climate zones is important for the dynamics of eddy momentum and heat transport and plays a crucial role in maintaining the mean state of the circulation (Walker and Schneider, 2006; Shaw and Pauluis, 2012). The Hawaiian Islands are located at latitudes that are influenced by the prevailing trade winds, strong vertical wind shear, and a persistent presence of a trade-wind inversion layer at elevations of 2000–2,200 m (Cao *et al.*, 2007; Longman *et al.*, 2015). During the boreal winter season, the trade winds are sometimes interrupted by the intrusion of upper level disturbances, cold fronts and subtropical cyclones (known as Kona lows, hereafter referred to as KL) that enter the sector of the Hawaiian Islands, which can result in significant rainfall events (Simpson, 1952; Kodama and Barnes, 1997; Kodama and Businger, 1998; Morrison and Businger, 2001). Although few in numbers in each winter season (Otkin and Martin, 2004a; Otkin and Martin, 2004b; Caruso and Businger, 2006), these extratropical disturbances contribute significant amounts to the annual rainfall over the Hawaiian Islands (Longman *et al.*, 2018). The trend analysis of gridded precipitation data (Frazier and Giambelluca, 2017; Frazier *et al.*, 2018) highlighted decreasing rainfall over the islands in recent decades. In addition, there is statistical evidence for an increase in dry days and decrease in heavy rain events (Chu *et al.*, 2010; Elison Timm *et al.*, 2011; Chen and Chu, 2014). These results motivated us to study how low-frequency variability in the North Pacific climate has affected the synoptic variability in the central subtropical Pacific. The focus of this article is how the dominant climate modes, including the El Niño—Southern Oscillation (ENSO), the Pacific-North American (PNA) pattern, the Pacific Decadal Oscillation (PDO), and the North Pacific Oscillation (NPO) have influenced the synoptic variability and rainfall in Hawai'i during the past decades. Furthermore, stationarity in the relationship between ENSO and KL activity is tested with respect to the change in the PDO phase during the mid-1990s.

The majority of extratropical storms move across the Pacific without penetrating deep into the subtropical Pacific. However, a number of cold fronts associated with elongated upper level troughs can reach the islands during the cold season (October to April). These extratropical disturbances sometimes transform into or initiate the formation of upper level lows, some of which induce the development of surface lows (Simpson, 1952). Otkin and

Martin (2004b, 2004a) studied the life cycle and interannual variability of KL events using 10-year reanalysis data. They found a strong connection between the extension of the Asian jet into the central and eastern North Pacific and the KL activity around the Hawaiian Islands. A zonally retracted jet that is accompanied by a westward shifted weaker Aleutian low favours KL activity during the cold season. Caruso and Businger (2006) extended the KL analysis using data for the period of 1980–2002. They found that the phases of ENSO affect the formation of KLs with increased frequency of KL during La Niña years.

In this paper we focus on the central North Pacific region and make use of a newly generated KL data product (Kaiser, 2014) with counts of upper level lows and lows penetrating through the troposphere down to sea level. The data are available from 1979 to 2014 and allow for the investigation of relationships between KL activity and the large-scale climate variability. Kaiser (2014) found 70 individual KLs formed during the Hawaiian cold season (October–April) in the years from 1979 to 2014. Furthermore, in that study it was shown that the frequency and intensity of KLs have significant impact on the interannual rainfall variability over the Hawaiian Islands. Analysis of daily precipitation data from windward and leeward stations on the islands revealed that the intensity and spatial distribution of rainfall over the Hawaiian Islands is markedly different during days with KLs compared with the predominant trade-wind induced precipitation. Associated with KLs west of the islands are moisture-laden the southwesterly winds—commonly referred to as “kona” winds in Hawaiian, though the Hawaiian culture has traditionally a much more diverse and nuanced wind classification scheme (Nakuina, 2005). They result in more precipitation along the dry sides of the islands, frequently with heavy rainfall intensities. This increases the average rain intensity more over dry leeward sites than in the wet windward regions.

It is evident that the climatic variations in frequency and the intensity of KLs are important for understanding interannual to decadal variability in Hawaiian rainfall pattern. Previous studies concentrated mostly on ENSO and PNA, which were considered most relevant for rainfall variability (Elison Timm *et al.*, 2011; O'Connor *et al.*, 2015; Frazier *et al.*, 2018). However, the effects of low-frequency variability associated with the PDO or Interdecadal Pacific Oscillation (IPO) are important for the global precipitation teleconnection pattern (Gershunov and Barnett, 1998; Hu and Huang, 2009; Dong and Dai, 2015; Li *et al.*, 2017; Dong *et al.*, 2018). At the same time, changes in the tropical ENSO system highlight a shift in the frequency of various types (or 'flavours') of ENSO (Ashok *et al.*, 2007; Kao and

Yu, 2009; McPhaden *et al.*, 2011; Johnson, 2013; Ren and Jin, 2013; Guo *et al.*, 2016), although it is still debated what processes lead to the development of ENSO flavours and if the observed changes constitute a change in the ENSO mode behaviour (Capotondi *et al.*, 2015; Capotondi and Sardeshmukh, 2017). In the light of this significant interaction between large-scale climate modes such as ENSO and PDO, it is important to develop a mechanistic understanding what controls regional precipitation patterns and how they may change in the future.

Within this larger research question, the results presented in this article provide a statistical analysis of the interannual variability in the large-scale climate modes and regional synoptic variability near the Hawaiian Islands. In this study, the linear relationship is studied between various modes of climate variability and the regional synoptic activity. To this end, time series indices of ENSO, PNA, and NPO are correlated with a regional index for synoptic activity based on potential vorticity variability, a rainfall index, and an outgoing longwave radiation (OLR) index (see Section 2). The central question addressed here is whether there has been a significant change in the teleconnection between ENSO and the regional synoptic variability over the Hawaiian region in the 1990s. Furthermore, the impact of decadal-scale PDO variability on the teleconnection pattern is investigated with composite analysis of the large scale circulation anomalies. Results of the data analysis are presented in Section 3, followed by a discussion in terms of statistical significance, and addressing the question to what extent the results are consistent with earlier studies that focused on decadal-scale changes in the Pacific climate system (Section 4). Section 5 summarizes the main results with concluding remarks.

## 2 | DATA AND METHODS

### 2.1 | Data sets

The study of KL activity in connection with modes of climate variability was based primarily on the data from the European Centre for Medium-Range Weather Forecasting (ECMWF) Re-Analysis (ERA) Interim project (Dee *et al.*, 2011). The data used are 6-hourly with a spatial resolution of  $2.5 \times 2.5^\circ$ . Sea level pressure (SLP), geopotential height at 500 hPa, and zonal winds at 250 hPa were averaged into monthly means and further averaged into cold season mean (April–Oct). Potential vorticity at 250 hPa was used to measure the strength of synoptic-scale variability (described below). Specific humidity at 700 hPa was used in connection with the analysis of the synoptic structure during KL events.

In addition, NOAA Interpolated OLR ([https://www.esrl.noaa.gov/psd/data/gridded/data.interp\\_OLR.html](https://www.esrl.noaa.gov/psd/data/gridded/data.interp_OLR.html)) gridded monthly mean data (derived from satellite remote sensing data [Liebmann *et al.*, 1998]) were used as an integrated measure of the radiative effects of optically thick clouds with high cloud tops. Over tropical oceans, OLR measurements are negatively correlated with precipitation (Tan *et al.*, 2013). However, in subtropical regions around Hawai'i, this relationship may be less robust, and hence OLR may not serve as a direct proxy for precipitation over Hawai'i. One reason is that significant rainfall amounts on the islands are a result of low-level clouds. These clouds emit long-wave radiation at similar temperatures as the surface (and the cloud-free low-level atmosphere). We use the OLR data set to define a regional OLR index for the Hawaiian Island region (see next section). Further, we use the gridded data set to inspect the local correlation between OLR and precipitation. This required a spatial interpolation of the OLR gridded data onto the precipitation grid. The software "Climate Data Operators" (CDO [version 1.7.1], Schulzweida (2019)) was used for bilinear interpolation of the OLR data.

Gridded monthly mean precipitation data from the Global Precipitation Climatology Project (GPCP; Version 2.3; <https://www.ncdc.noaa.gov/cdr/atmospheric/precipitation-gpcp-monthly>) were downloaded and seasonal averages for the October–April seasons were calculated. Rainfall anomalies in this study are expressed as percentage differences with respect to the 1981–2010 climatological mean.

### 2.2 | Indices

The following indices are used to represent the dominant modes of North Pacific climate variability. For ENSO, we chose two separate indices in order to investigate the tropical SST impacts on the central subtropical Pacific region around Hawai'i. The monthly mean SST-based Niño3.4 index ( $5^\circ\text{S}$ – $5^\circ\text{N}$ ,  $120$ – $170^\circ\text{W}$ ) was obtained from the National Oceanic and Atmospheric Administration (NOAA) (<http://www.esrl.noaa.gov/psd/data/correlation/nina34.data>), and monthly mean El Niño Modoki index (EMI) (Ashok *et al.*, 2007) was obtained from the Japan Agency for Marine–Earth Science and Technology (JAMSTEC) (<http://www.jamstec.go.jp/frsgc/research/d1/iod/DATA/emi.monthly.txt>). The Pacific Decadal Oscillation index (PDO) was obtained from NOAA (<https://www.ncdc.noaa.gov/teleconnections/pdo/>). All time series were converted into cold season averages (Oct–Apr) for the comparison with the regional synoptic activity in each season. Our primary data analysis is

based on the years 1980–2014, however, statistical analyses are limited to the years 1980–2012 when the Hawaiian Islands rainfall index or the OLR index is used (see below). In the text we refer to a cold season Oct–Apr by the year of the month January. For example, the cold season during El Niño event 1997/98, is assigned the year 1998.

In addition to these SST-based indices, atmospheric circulation variability over the extratropical North Pacific is represented by the Pacific–North American Pattern (PNA) index (as defined and distributed by the NOAA Climate Prediction Center's (CPC) ([http://www.cpc.ncep.noaa.gov/products/precip/CWlink/pna/pna\\_index.html](http://www.cpc.ncep.noaa.gov/products/precip/CWlink/pna/pna_index.html))). The North Pacific Oscillation (NPO) index was calculated using the monthly mean SLP data following the method described in Yu and Kim (2011). Principal Component Analysis (PCA) was applied to the SLP data within the domain of 20–60°N and 120–280°E. First, the long-term mean climatological cycle during 1980–2014 was subtracted for each month. Next, the PCA was calculated based on the covariance matrix. The second mode is then used to create the seasonal mean NPO index from the monthly principal component index series.

Important for the climatic analysis of synoptic weather activity is to define an index that measures the average activity during a cold season. For this purpose, we started initially using the number of days with KLS in each cold season as a measure of KL activity. The numbers of KL days are based on the work of Kaiser (2014) using a revised version data set with KL event dates (Kaiser 2015, pers. communication, unpublished data). The KL index (KLI) is the sum of all days with a KL present in a season. This index does not separate individual storm events or the duration of single events. It is noted that we obtained a slightly modified KL event data set compared with the tabulated data of Kaiser (2014). In this version two KL events were re-classified later while conducting a daily rainfall analysis for the Island of Oahu (Dr. Ryan Longman, University of Hawai'i at Mānoa, pers. communication). These events coincided with frontal systems that were previously classified as closed cyclonic systems at sea level. The front analysis was based on the regional analysis of objectively identified fronts (Berry *et al.*, 2011). Figure 1 gives two illustrative examples of two well-developed KLS with centres northwest and northeast of the islands. It highlights the importance of KLS for the advection of tropical moisture across the islands and the presence of the upper level vorticity anomalies.

The cumulative counts of KL days have several disadvantages for the statistical analysis of synoptic weather activity over the Hawaiian Islands. First of all, the current KL event data set is based on individual partly

subjective interpretation of the circulation pattern and prone to errors. Second, the application of hard thresholds for the classification of weather systems that leads to event counts is sensitive to threshold parameters. Furthermore, many aspects of the synoptic variability may not be well represented by the count statistic alone. Therefore, it was decided to work with an additional measure of synoptic-scale variability that is derived by band-pass filtering atmospheric circulation fields in the synoptic frequency range.

Since upper level advection of potential vorticity plays an important role in the development of KLS (Morrison and Businger, 2001), a regional PV activity index (PVI) for the Hawaiian Island region was created as follows. For each cold season, 6-hourly 250-hPa PV data were band-pass filtered for 8-16-day variability (using Fast Fourier Transformation [FFT]), and the band-pass filtered variance was calculated for each cold season (Oct–Apr). Note that 8-16-day time scale is more appropriate for the subtropical storm systems, which show rather erratic and slow movements in this region of the Pacific (Otkin and Martin, 2004a).

Initially two regions were tested in which the PV activity was measured: a western region relative to the main Hawaiian Islands extending from 15 to 30°N and 170 to 160°W, and an eastern region from 15 to 30°N and 160 to 150°W (see Figure 1). In this study, the average from both regions is used.

For the comparison with rainfall variability over the Hawaiian Islands we obtained the Hawai'i Rainfall Index (HRI) that was developed by means of geospatial statistical methods that filled gaps in the station network and interpolated the point data to a homogeneous grid (Frazier *et al.*, 2016; Frazier and Giambelluca, 2017). The wet season index was available up to the year 2012 at the time of this study, which restricts the statistical data analysis in connection with the HRI to the years 1980–2012. The relationship between Hawaiian rainfall and OLR is investigated with a regional OLR index that was calculated by averaging the gridded data over the geographic domain (15–30°N, 170–150°W) using the years 1980–2012.

### 2.3 | Statistical methods

The statistical analysis is based on linear correlation analysis and tests for differences in the Pearson's correlation coefficients between two time intervals before and after the mid-1990s. Statistical significance test was applied with block bootstrapping methods for time series (Davison and Hinkley, 1997). The purpose of the block-wise resampling is to maintain the autocorrelation within individual time series and thus maintain the effective

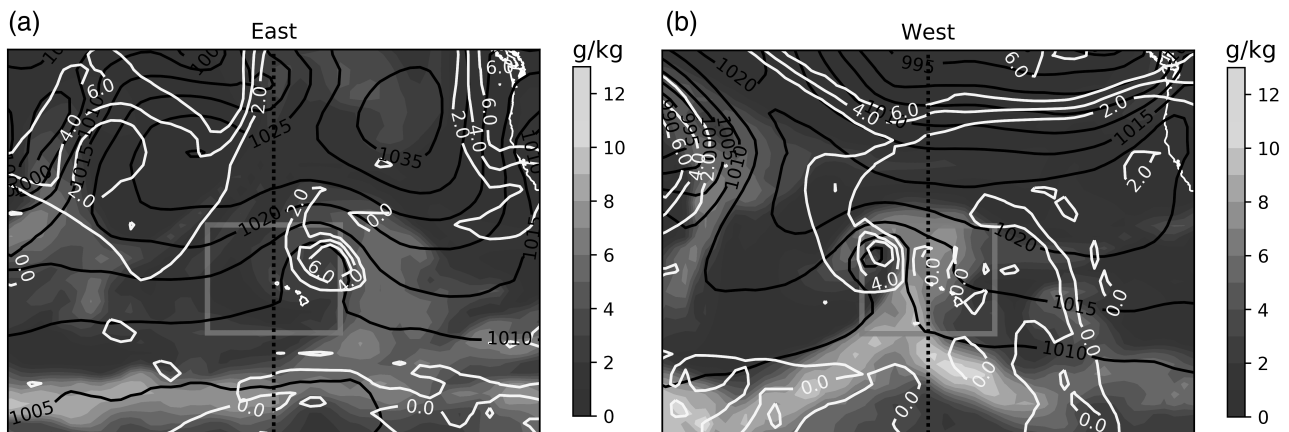


**FIGURE 1** Two examples of Kona low (KL) events: (a) KL east off the islands on date December 10, 2012 (b) KL west of the islands on date November 28, 1999. White yellow contours show the potential vorticity at 250 hPa (units for the 250 hPa are PVU), black contour is SLP (hPa), and the shaded area is specific humidity at 700 hPa ( $\text{g}\cdot\text{kg}^{-1}$ ). The grey squares in these two figures mark the grid domain used for the PV index calculation

sample size. In our approach we resample the paired data from the full time series using the same sample sizes as in the pre-and post-shift sub-periods. The correlation coefficient is calculated for these two randomly subsampled data sets, from which we obtain the difference between the two correlation coefficients. The bootstrap replications were done with the function ‘tsboot’ from the package ‘boot’ (Davison and Hinkley, 1997; Canty and Ripley, 2017) using R (R Core Team, 2015). The results are based on 1,000 replications with a fixed block width of  $L = 5$ . Sorting the 1,000 differences in the correlation coefficients gives us the estimates for the confidence intervals and allows us to estimate the  $p$ -value for the difference in pre-and post-shift correlation. We note that we conducted the same resampling tests with smaller ( $L = 3$ ) and larger blocks ( $L = 7$ ). The results showed that the estimated confidence ranges and the derived  $p$ -values for the null hypothesis were robust.

We also applied resampling methods for testing the significance in the windowed correlation analysis (see Figure 5). A sliding data window of 11 years is used to look at the temporal changes in the correlation between two time series. The resulting correlation coefficient is compared with the two-sided 90% confidence intervals under the null hypothesis that the two time series are uncorrelated. To this end, we resampled the two time series with a random temporal lag between the two data windows. The offset in the starting point of the windows was varied between 1 and 5 years in order to test the effects of serial correlation on the confidence intervals. Each time 1,000 randomly paired windows were used to calculate correlation coefficients. From this empirical distribution of the correlation coefficient we obtained the fifth and 95th quantiles. The results reported in this study are robust against the choice of the lag-constraint.

In addition, we deployed a regime shift detection method (Rodionov, 2004; Rodionov and Overland, 2005) on the windowed correlation time series to support the timing of the change in the correlations. We used code developed for R (Stirnemann *et al.*, 2019). These auxiliary tests are presented in the SI material (Table S1, Figure S3).

Composite maps that highlight differences in the means are presented. Here the focus is on differences between El Niño events during positive and neutral/negative PDO phase. The composites for the La Niña events in relation to the PDO phase are provided in the SI material. The years used for the composites are listed in Table 1. We report these maps without strict tests for statistical significance due to the small sample size. The SI material provides results with Monte-Carlo simulations in which the composites are calculated based on randomly sampled years. Multidimensional Scaling (MDS) was applied to compare the magnitude of differences obtained by the random Monte-Carlo composites with the PDO-based composites. The results give an estimate for the probability of obtaining by chance differences in the composite maps less or equal to the size of those found in the PDO-based composites. Throughout the text, however, we exercise caution in the interpretation of the results since the statistical significance of the pattern differences must be considered low due to the small sample sizes.

### 3 | RESULTS

This section presents the statistical analysis of the large-scale climate variability and regional synoptic activity measured by the KLI and the PVI. The major results suggest a change in the impact of El Niño on synoptic activity near Hawai’i during the past decades.

**TABLE 1** List of years used in the composite analysis

ENSO\PDO	Positive PDO index (+PDO)	Negative PDO index (-PDO)
<b>El Niño (+ENSO)</b>	1983, 1987, 1998, 2003	1992, 1995, 2005, 2007
<b>La Niña (-ENSO)</b>	1985, 1986	1999, 2000, 2001, 2008, 2009, 2011, 2012

Note: Rows discriminate El Niño and La Niña events, columns the phase of the PDO. The analysis was limited to the ERAinterim reanalysis data period starting in 1979 (and ending in 2014 due to availability in the KL data set). Note that the year refers to the January month during the peak season, which usually spans the winter season DJF. It is noted that La Niña events are listed here to complement the table. However, this study is focused on the El Niño\PDO events.

First, the linear regression statistics and the stability of the correlations are presented. Second, a composite analysis of large-scale circulation pattern is presented. Emphasis is put on the differences in circulation anomalies associated with El Niño events and changes in the PDO from positive to more negative/neutral conditions.

### 3.1 | Linear relationships among indices of regional synoptic variability near Hawai'i

This section compares different types of regional climate indices, which provide a measure of synoptic-scale variability and rainfall variability during the season October through April. The correlations ( $r$ ) are reported here for the two time periods which are referred to as 'pre' (1980–1994) and 'post' period (1995–2014, or 1995–2012 when the regional OLR index or the HRI is used in the analysis). The significance of the differences in correlations was estimated by means of resampling methods described in Section 2.3.

A positive correlation is found between KLI and PVI (Figure 2) with a correlation of  $r = .58$  for the period of 1980–2014. The correlation during the pre-shift period was slightly stronger ( $r = .69$ ) than that of the post-shift period ( $r = .50$ ) but the changes are not statistically significant ( $p > .10$ ). A robust positive correlation can be found between the PVI and the HRI throughout the years (Figures 2 and 3), with some increase in the correlation in the post-shift years (pre-shift  $r = .53$ , post-shift  $r = .72$ ,  $p > .10$ ). These correlations show that the synoptic-scale activity measured by the PVI is an important factor for the interannual rainfall variability in Hawai'i. The KLI itself has a lower correlation with

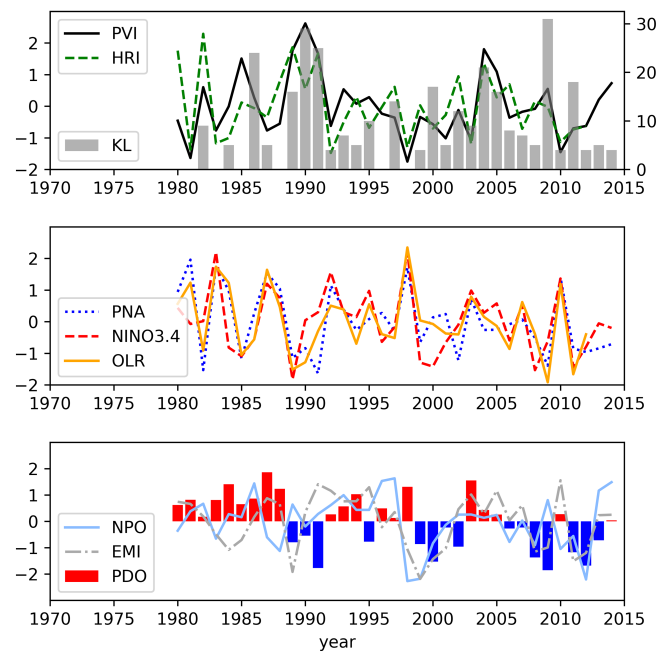


**FIGURE 2** Time series of the seasonal potential vorticity activity index (PVI), Hawaii rainfall index (HRI), and Kona low index (KL, top). The index labelled 'KL' (grey bars) depict the updated KL event counts of this study, KL\_14 (crosses) show the original data from Kaiser (2014). Large-scale modes of variability indices for PNA and ENSO (NIÑO3.4 SST index), and the regional outgoing longwave radiation index (middle); North Pacific oscillation (NPO), ENSO Modoki index (EMI) and the Pacific decadal oscillation index (PDO) (bottom). Note all indices except the KL indices have been centred and scaled (z-scores). HRI index is for the wet season November–April, other indices are Oct–April seasonal means

HRI. This was expected because (a) KL events are few in numbers during the season, and (b) they exclude frontal passages. Furthermore, the semi-objective classification method is prone to errors and classification uncertainties. For example, identification of the closed isobars that indicates a low-pressure system at the surface depends on the visualization tools applied. We tested the sensitivity of the results that are based on our updated KL event data set by comparing it with the results based on the KL events of Kaiser (2014). As can be seen in Figure 2, the results are very similar. However, the PVI is preferred over the KLI as a regional index for synoptic activity in the following discussions.

The measure of synoptic activity using the PVI shows strong negative correlation with the regional OLR index. High values of synoptic PV variability in the upper atmosphere indicate the influence of extratropical air masses penetrating the subtropical latitudes, which can induce more cloud formation in the upper

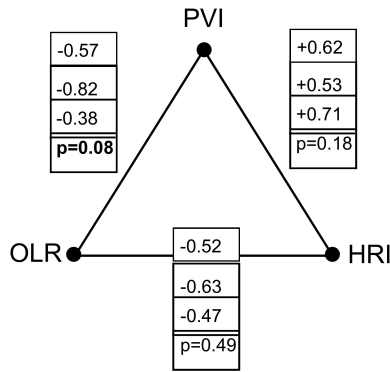


**FIGURE 3** Schematic summary of the correlations between synoptic activity (PVI) outgoing longwave radiation (OLR) and Hawaii rainfall index (HRI). For each connecting line between the vertices the correlation is tabulated for the all years, pre and post period (order from top to bottom). The significance test for differences in the correlation is shown in the lowest box at the bottom of the column. Bold-faced are  $p$ -values ( $p < .1$ ) that highlight weak evidence against the null hypothesis ( $H_0$ : No change in correlation)

troposphere or deep convection. Compared with the prevailing shallow and warm trade-wind clouds, the average OLR is to be expected to be lower in seasons with high PV variability.

Comparing the correlation between regional OLR and PVI (see Figure 3), it is seen that the negative correlation has decreased significantly in recent years (from  $r = -.82$  to  $r = -.38$ ,  $p < .1$ ), whereas the correlation between HRI and PVI has remained at similar levels ( $r = .53$ ,  $r = .71$ ,  $p > .1$ ). Likewise, the relationship between OLR and KLI remained at the same level ( $r = -.56$ ,  $r = -.58$ ). A small reduction in the correlation between OLR and HRI is indicated but not statistically significant (Figure 3). Since the changes in regional correlations are not statistically significant when applying more conservative significance test of  $p < .05$ , it is questionable whether a physical mechanism was the cause for the changed relationship between regional PVI and OLR. Further insight can be gained from the correlation between OLR and precipitation over the wider domain of the North Pacific, which provides additional support that rainfall mechanisms during the cold season have changed. In Figure 4 it can be seen that over the subtropical central Pacific and the eastern sector the correlation between OLR and precipitation was stronger in the pre-shift years compared with the post-shift years. This indicates a change in the cloud types or the rainfall mechanisms.

In summary, the regional climate indices provide evidence that the local rainfall variability during the wet

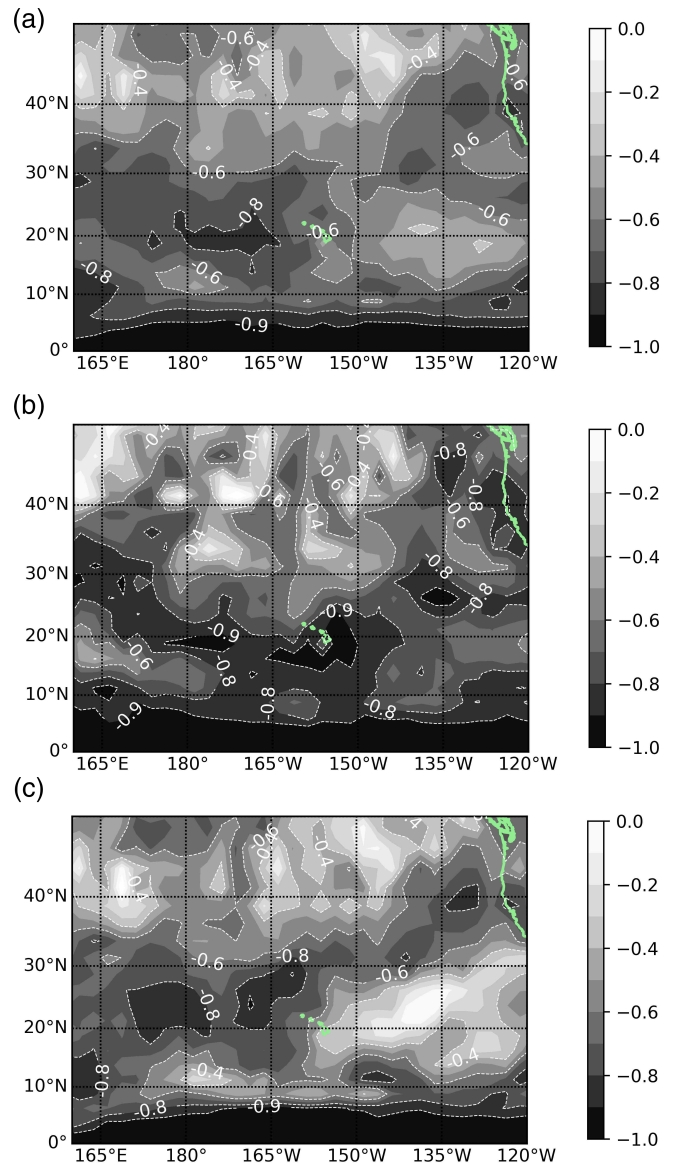


**FIGURE 4** Map with the local correlation coefficients between OLR and GPCP precipitation time series. Top (a) shows the correlation for all years 1980–2014, middle (b) is the correlation for pre-shift years, and bottom (c) figure shows the correlation for the post-shift years. Correlations were calculated using Oct–Apr seasonal mean data

season is largely depending on the regional synoptic storm activity. The correlation between rainfall and synoptic activity is robust in time. The negative correlation between OLR and rainfall is relatively stable, suggesting that OLR can serve as a proxy for rainfall variability over Hawai'i. However, the relationship between the regional OLR and synoptic activity was weaker in the recent years compared to the years prior to the mid-1990s.

**TABLE 2** Correlation results for the regional indices representing synoptic activity (KLI and PVI), cloudiness (OLR index), and rainfall (HRI) index with large scale circulation indices

	NIÑO3.4	Modoki	NPO	PNA
KLI	-0.24	+0.01	+0.23	-0.50
	-0.28	+0.05	+0.24	-0.55
	-0.20	-0.02	+0.27	-0.45
PVI	-0.30	+0.04	+0.39	-0.67
	-0.54	-0.29	+0.23	-0.88
	-0.16 <	+0.22	+0.49 >	-0.57 < <
HRI	-0.30	+0.03	+0.22	-0.61
	-0.37	-0.07	-0.02	-0.72
	-0.34	+0.05	+0.37 >	-0.56 <
OLR index	+0.72	+0.30	-0.32	+0.85
	+0.64	+0.24	-0.42	+0.89
	+0.78	+0.33	-0.35	+0.83

*Note:* The correlation coefficients are reported as triplets, where the first (top) value refers to the correlation using the years 1980 to 2014 (2012 for rainfall and OLR indices), the middle is for the pre-shift years to 1980–1994 (middle), and for the post-shift years from 1995 to 2014 (2012) (bottom). Significant differences in the correlation coefficients between the two time periods are marked with “<<” (“>>”) for reduced (increased) strength in correlation from pre to post-shift period. Significance was estimate using time series bootstrapping with R package tsboot. A single ‘<’ ‘>’ indicates noteworthy changes in the correlation that did not pass the significance test, though.

## 3.2 | Linear relationships between regional indices and climate modes

### 3.2.1 | ENSO

Rainfall in Hawai'i has been studied in connection with ENSO variability in depth (Chu, 1995; Chu and Chen, 2005; Alison Timm *et al.*, 2013; O'Connor *et al.*, 2015; Frazier *et al.*, 2018). Our results confirm the impact of El Niño and La Niña events on the wet-season rainfall with below and above average values in the rainfall index. The linear correlation coefficient between NIÑO3.4 and HRI is relatively weak when calculated for the pre and post shift period ( $r = -.37$ ,  $r = -.34$ , respectively); stronger correlations are found between HRI and PNA ( $r = -.72$ ,  $r = -.56$ ; see also Table 2). The predominant influence of PNA is consistent with results in Frazier *et al.*, 2018. Given the importance of synoptic disturbances for the wet-season rainfall over the Hawaiian Islands, it is worth studying the impacts of ENSO on the PV activity. A closer inspection of the time series indicates a shift in the relationship between PVI and NIÑO3.4 index during the 1990s, which can be seen in the scatter plot of NIÑO3.4 and PVI (Figure 5) using two sub-sampled

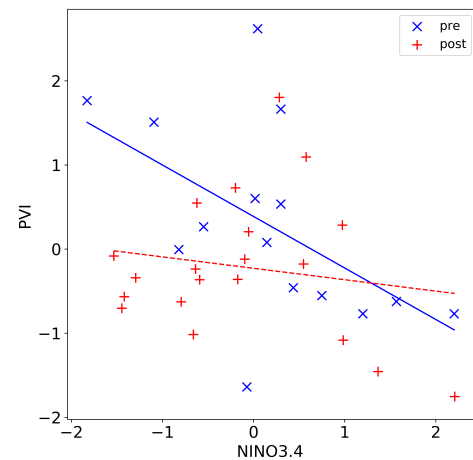


**FIGURE 5** Scatter plot for NIÑO3.4 (x-axis) and PVI (y-axis); markers ‘x’ indicate data from years up to 1994, ‘+’ signs mark the years after 1994. The linear regression line for the pre-1995 period is shown in as solid line ( $r = -.54$ ), the dashed line is for the post period ( $r = -.16$ )

groups with years 1980–1994 (pre-shift period) and the years after 1994 (post-shift). In the pre-shift period this ENSO - PVI connection was more pronounced than in the post-shift period. The linear regression lines fitted to the pre and post period data highlight the weakened correlation in recent years. Prior to 1995, the relationship between Niño3.4 and PVI has a significant negative correlation ( $r = -0.54$ ), whereas in post-shift years the correlation is much weaker ( $r = -0.16$ ) and insignificant.

The transition in the NINO3.4 - PVI correlation is also seen in the moving 11-year window correlation analysis shown in Figure 6. At the same time the correlation between PVI and the NPO index has increased (though not statistically significant), which indicates that the teleconnection between tropical and subtropical/extratropical modes of climate variability have fluctuated over time. In Section 4 we discuss the statistical results in the context of tropical-extratropical interaction mechanisms that have been studied in relation to decadal-scale climate variability or climatic shifts.

Since the structure and position of tropical Pacific SST anomalies have an impact on the atmospheric teleconnection pattern, we also considered the ENSO Modoki index (EMI) in connection with the local impacts over Hawai'i in terms of synoptic activity. The strength of the correlation between EMI and PVI is weaker in general and below the significance level, with a change from  $-0.29$  (pre-shift) to  $+0.22$  (post-shift period). The low correlation values with the Hawaiian rainfall indices is somewhat surprising at first, but it matches with previous studies that have



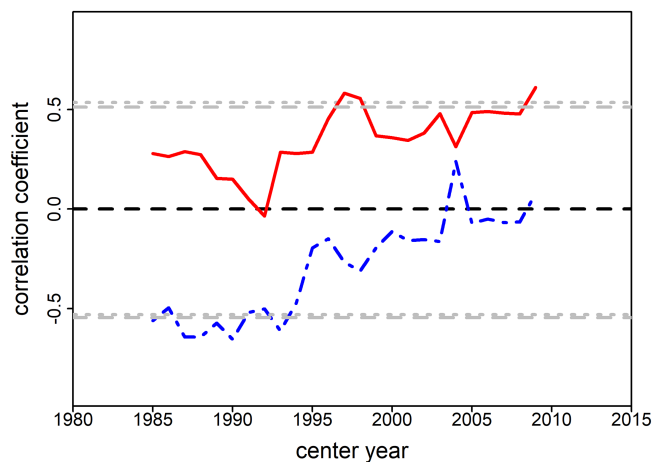


**FIGURE 6** Windowed correlation analysis. Shown is the correlation between PVI index and NINO3.4 index (dash-dotted line), and the correlation coefficient between PVI and NPO index (solid line). The values are assigned to the centre year of the 11-year window. 10%- two-sided significance levels shown as grey dash-dotted lines were estimated by a bootstrap resampling method (see Section 2.3)

shown the CP mode produces a teleconnection pattern with low signal amplitude located over Hawai'i (Ashok *et al.*, 2007). The role of central versus eastern Pacific SST anomalies in connection with changes in the relationship between ENSO and Hawaiian rainfall will be discussed in Section 4 in more detail.

### 3.2.2 | PNA and NPO

The PNA pattern is closely related to the first EOF mode of the SLP variability in the North Pacific. The connection between ENSO and PNA is relatively strong and has changed little between pre and post-shift period. The second EOF mode of the SLP variability corresponds to the NPO, and therefore it is weakly correlated with the PNA index ( $r = -.35$  and  $r = -.27$  for pre- and post-shift period; see also Figure 7). The influence of the PNA variability on Hawai'i's synoptic activity as measured by the PVI was very strong before the 1990s and then experienced a significant decline (from  $r = -.88$  to  $r = -.57$ ,  $p < .1$ ). A slight reduction in the linear relationship with the Hawaiian rainfall index is also observed, while the connection of PNA with OLR remained the same (Table 2).

The NPO index plays a lesser role than the PNA in influencing the synoptic activity around Hawai'i on interannual time scales. On the decadal time scales, the NPO has undergone a transition from positive into

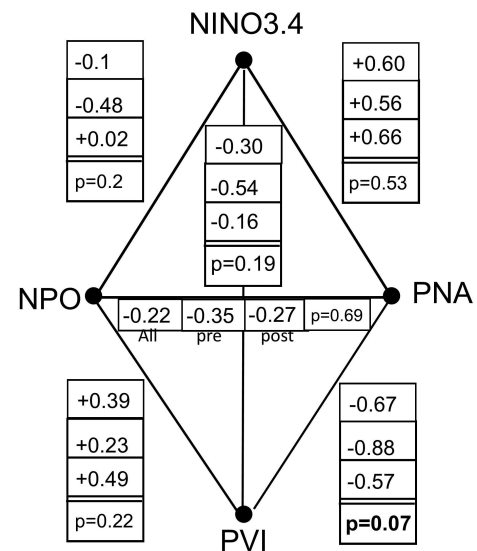


**FIGURE 7** Summary of the correlations among the leading modes of large-scale variability (ENSO, NPO, and PNA) and their relation to the local synoptic activity in Hawaii (PVI). For each connecting line between the vertices the correlation is tabulated for all, pre-shift, and post-shift years (order from top to bottom; left to right for the NPO-PNA correlation analysis). The significance test for differences in the correlation is shown in the lowest box at the bottom of the column. Bold-faced are  $p$ -values ( $p < .1$ ) that highlight evidence against the null hypothesis ( $H_0$ : No change in correlation)

negative phase (Yu *et al.*, 2012a), which coincides with the mid-1990s shift found in this study. Moreover, the spatial dipole pattern associated with the NPO has shifted eastwards (obtained by regressing the North Pacific SLP data onto the NPO index), which affected the strength of the teleconnection over North America (Sung *et al.*, 2019). Over Hawai'i one can observe an increase in the correlation between NPO index and PVI in the post-shift period.

The analysis of the correlations among the regional circulation indices and climate modes suggest that the observed changes between NIÑO3.4 and local synoptic variability is a result of changes in the extratropical North Pacific circulation. ENSO's influence on the synoptic variability decreased at the same time as the impacts of NPO variability became more influential on the rainfall (and synoptic activity) in Hawai'i (Figure 7 and Table 2). Whereas the PNA variability maintained a direct influence on the PV activity, the overall correlation strength dropped due to the competing influence of the NPO-type circulation variations. In the next section we concentrate on the North Pacific upper level winds and geopotential height anomalies. The large-scale circulation anomalies provide supportive information that help to explain the regional changes around Hawai'i that have been presented here.

### 3.3 | Composite analysis of the large-scale circulation

During 1990s the PDO index changed from positive to predominantly negative phase, although there is not a high-amplitude signal on multidecadal time scales associated with this recent phase transition (see Figure S1). The timing of this transition coincides with the change in the correlation between large-scale circulation indices and local synoptic PV variability over Hawai'i. The composite analysis in this section takes a look at the atmospheric circulation anomalies during El Niño years separated in two groups based on the positive and negative phase of the PDO index. It should be noted that uncertainties in observations of Pacific SST and choices in the data processing could result in uncertainties that affect the amplitude and timing of the phase transition in the PDO index Wen, Kumar and Xue (2014). This type of uncertainty has not been accounted for in this study. Based on the results that Wen, Kumar and Xue (2014) presented in their Figure 4, we argue that the main conclusions drawn from our results are robust against errors of that magnitude, since they do not change the overall temporal character of the PDO variability. The choice of the climatological reference period, as well as the application of time series signal processing for standardization of the PDO index, can affect the sign of the PDO index. Our composites are based rather on the ranks of the PDO index values instead of strict sign-based selection criteria (see scatter plot in Figure S2 for illustration).

The results presented here mainly focus on the El Niño events (+ENSO). Table 1 lists the years of the four possible ENSO/PDO state composites. Interested readers can find similar figures with composites of La Niña (−ENSO) events and the two PDO phases in the SI Figures S8 to S10.

The sample size is small given the constraints on the data used here. Arguably, parametric tests for significant differences would suffer from the limited sample size. Furthermore, without taking into account the problem of testing for field significance highlighting areas of significance in composite differences could result in a too optimistic depiction of the significance (Wilks, 2016). Therefore, the comparison of the circulation anomalies between El Niño events during positive and negative PDO are done qualitatively without formal significance tests. In an attempt to measure how unusual the differences are between the two composites, we reduced the pattern difference into a simple scalar metric, the Euclidean distance. Monte Carlo sampling was then applied to generate 200 random composite differences. The distance calculation is done with the support of Multidimensional Scaling (MDS) for a visual illustration

of the random pattern differences and those of the actual composite.

The results show that the difference between the El Niño years with positive PDO (+ENSO/+PDO) and the negative PDO El Niño years (+ENSO/−PDO) is not exceptionally large. About 50% of the random composites produce distances equal to or greater than the specific difference in our two groups. However, one has to remember that the subsampling is done with El Niño years, so we would not expect as large a difference as for example in the case of El Niño to La Niña years. Some similarity in the overall El Niño 500 hPa response pattern over the North Pacific is connecting the PDO positive and negative composite subgroups (see SI text and Figures S4–S5 for additional information).

Upper level zonal wind patterns during El Niño events show significant strengthening and eastward extension of the mid-latitude jet compared with the long-term mean state. The composite analysis (Figure 8) shows that the strengthening of the zonal wind jet at 250 hPa level during the El Niño years with positive PDO (+ENSO/+PDO) is stronger than during the El Niño with negative PDO (+ENSO/−PDO). The differences between +ENSO/+PDO and +ENSO/−PDO composite anomalies are located in the central and eastern sector over the North Pacific. The composite maps show a weakening of zonal wind north and northeast of the Hawaiian Islands during negative PDO phase. Since synoptic wave disturbances are steered by the position of the upper level zonal jet, the changes indicate that the extra-tropical storms are usually moving across the Pacific towards the North American continent during El Niño years. The recent negative phase of the PDO, however, indicates that the exit region of the jet is located more in the central Pacific, reducing the organized wave activity flux into the eastern North Pacific. In addition, the composite analysis with respect to La Niña events suggests that the largest differences in the zonal wind pattern are shifted more towards the western sector (Figure S9).

The 500 hPa geopotential height anomalies depict a pattern consistent with the zonal wind anomalies. A weakened geopotential anomaly over the North Pacific during +ENSO/−PDO events is observed. The centre of this difference in the ENSO teleconnection pattern is not projecting directly onto the centres of action seen in the PNA pattern, which could explain why the correlation between NIÑO3.4 and PNA index has not changed significantly (Figure 7). This pattern is consistent with a shift in the centres of action in the NPO found by Sung *et al.* (2019). The authors of that study pointed out that changes in the baroclinicity in the western Pacific have an impact on the eddy-mean flow interactions downstream. It is therefore possible that the anomalies in the strength and position of the zonal jet is linked to the SST

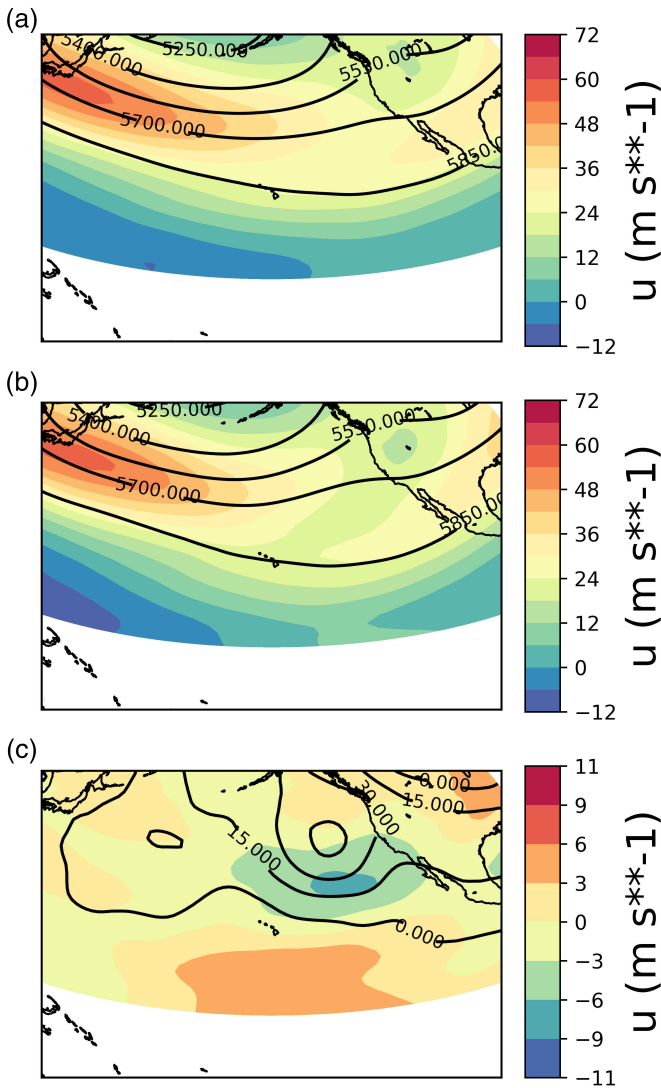


**FIGURE 8** Upper level zonal wind at 250 hPa (shaded colours) and 500 hPa geopotential height fields (contours in m). Top panel is for years (+ENSO/+PDO), middle panel for years (+ENSO/-PDO). Bottom figure shows the difference (+ENSO/-PDO) minus (+ENSO/+PDO), where shadings indicate stronger westerlies in red and weaker westerlies in blue during El Niño years with negative PDO compared with El Niño years and positive PDO. All data refer to the cold season Oct–Apr

anomalies in the western tropical Pacific. The shift in the zonal jet and the corresponding geopotential height anomalies could also be a response to the changes in the spatial pattern of the El Niño SST anomalies. Three of the four +ENSO/+PDO years were EP events; in contrast three of the four +ENSO/-PDO years were CP events (Yu *et al.*, 2012b). The consequence of this systematic retraction of the upper level jet is a diminished steering effect of El Niño on the extratropical disturbances and their pathways north of the Hawaiian sector during negative phase of the PDO.

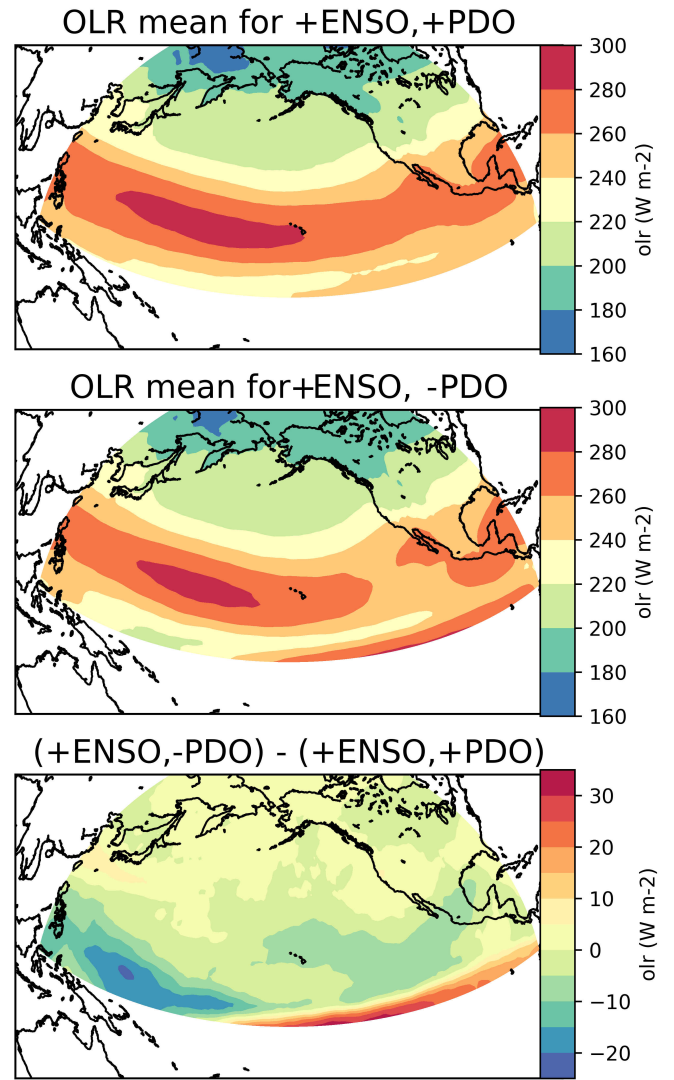


**FIGURE 9** Outgoing longwave radiation (OLR; shaded colours). Top panel is for years (+ENSO/+PDO), middle panel for years (+ENSO/-PDO). Bottom figure shows the difference (+ENSO/-PDO) minus (+ENSO/+PDO), where shadings indicate more (less) OLR in red (blue) during El Niño years with negative PDO compared with El Niño years and positive PDO. All data refer to the cold season Oct–Apr

The OLR composites are shown in Figure 9 together with the differences between negative PDO El Niño years and positive PDO El Niño years. The largest signals are found over the tropical Pacific, indicating the connection between tropical forcing and extratropical circulation. A small negative anomaly is seen in the OLR over Hawai'i and parts of the central subtropical North Pacific. The negative OLR values indicate that the upwelling flux of long-wave radiation from the warm ocean surface and warm low troposphere was more effectively blocked by 'cold' clouds since the mid-1990s (during El Niño events).

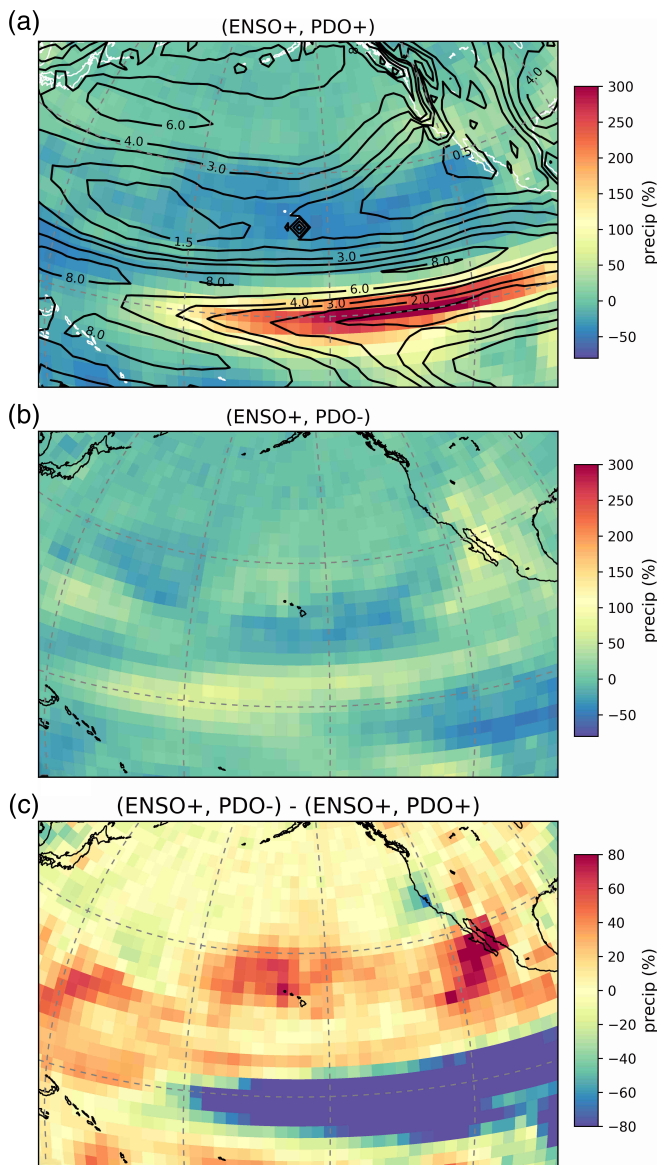


**FIGURE 10** Precipitation anomalies relative to the climatology (1981–2010) expressed in percentages (shaded colours). Climatology is shown in contours in the top figure in unit  $\text{mm}\cdot\text{day}^{-1}$ . Top panel is for years (+ENSO/+PDO), middle panel for years (+ENSO/-PDO). Bottom figure shows the difference (+ENSO/-PDO) minus (+ENSO/+PDO), where shadings indicate more (less) precipitation in red (blue) during El Niño years with negative PDO compared with El Niño years and positive PDO. All data refer to the cold season Oct–Apr

However, the correlation analysis between precipitation and OLR over the North Pacific (Figure 4) indicated already that the interpretation of OLR as a proxy for precipitation outside the tropics has to be considered with some caution. Therefore, a similar composite analysis was conducted with the GPCP rainfall data. The pattern in the differences between the two El Niño composites

(Figure 10) shows the rainfall anomalies over the central subtropical North Pacific including the Hawaiian Island region have been more negative during the positive PDO phase, which is consistent with the OLR composites.

## 4 | DISCUSSION

This study analysed the statistical relationships between large-scale climate variability in the North Pacific and synoptic activity in the central subtropical Pacific over the Hawaiian Islands.

It was shown that synoptic activity associated with extratropical storms is a main contributor to the inter-annual rainfall variability over the Hawaiian Islands. Our results support the recent finding of Frazier *et al.*, (2018) that ENSO and PNA variability are important for the inter-annual rainfall variability over the subtropical Hawaiian Islands during the cold season months. However, the results indicate a multidecadal modulation of the correlations between regional synoptic activity in the central subtropical Pacific and the large-scale climate modes.

In the following we discuss the statistical results together with the potential physical mechanisms that could explain the observed changes. It should be kept in mind that the statistical results are overall marginally significant. This is partly due to the small sample sizes and partly due to the weak signal-to-noise ratio. We discuss here two important questions: (a) is there additional support for our claim that PDO phases modulate the strength of ENSO teleconnection pattern in the North Pacific sector, and (b) how important are changes in the NPO that coincide with the PDO phase change during the 1990s?

The composite analysis of the upper level zonal winds provided evidence for a systematic shift in the zonal jet structure during the mid-1990s in connection with multidecadal climate variability. The composite analysis of El Niño events showed that the positive phase of the PDO reinforces the impact of ENSO variability on central Pacific storm track variability. With the strengthened and extended zonal jet synoptic disturbances steered towards the North American continent away from the Hawaiian Islands (Seager *et al.*, 2010; Winters *et al.*, 2019), and consequently synoptic activity was more effectively reduced during the positive PDO phase. Some additional quantitative support can be found in the SI material in Figure S6 and S7.

During the post-shift years with more frequent negative PDO the weaker jet stream constitutes a less organized wave guide in the central Pacific. In this state, the jet allows increased ‘leakage’ of extratropical disturbances into the subtropics (Seager *et al.*, 2010). This enhances the probability of cut-off low formation near

Hawai'i (Chu and Chen, 2005; O'Connor *et al.*, 2015). The results shown here suggest that the impacts of El Niño (and La Niña) events for Hawai'i's winter weather depend in part on the mean position and strength of the mid-latitude jet. Otkin and Martin (2004b) indicated that the stationary wavenumber Ks calculated from the upper level zonal wind can be used as waveguide for synoptic disturbances. Their results indicated that a weakening of the zonal wind jet increases the probability of KL occurrence near Hawai'i. In addition, independent modelling studies with prescribed SST anomalies that represent conditions of El Niño and La Niña years during positive and negative IPO phases (Dong *et al.*, 2018) are consistent with our main conclusion that interdecadal changes in the PDO (or IPO) have impact on storm track variability over Hawai'i.

The most noticeable difference in the correlation strength was found between PNA and PVI, with a weaker linear relationship in the post-shift period than in the pre-shift years. Similar changes were found in the PVI-NIÑO 3.4 correlation, though without passing the statistical significance test. The observed changes in these two latter bivariate correlations coincide with an increase in the correlation between PVI and NPO index. Furthermore, the dominant ENSO mode shifted from the eastern Pacific (EP) mode into the central Pacific El Niño (CP) mode, though with considerable uncertainty in the timing when the change took place (Larkin, 2005; Ashok *et al.*, 2007; Kao and Yu, 2009; Kug *et al.*, 2009; McPhaden *et al.*, 2011; Johnson, 2013; Xiang *et al.*, 2013; Capotondi *et al.*, 2015; Capotondi and Sardeshmukh, 2017). As to the causes of multi/decadal changes in the tropical-extratropical ocean-atmosphere system, multiple interacting mechanisms could be responsible. On seasonal timescales the NPO is one important link between extratropical atmospheric circulation and tropical SST anomalies. Yu and Kim (2011) suggested that during the decay phase of EP ENSO events, the associated extratropical SLP anomalies shift from the first SLP mode (that is PNA) to the second SLP mode (NPO). They concluded that extratropical SLP variations play an important role in exciting the CP event type of ENSO through the seasonal footprinting mechanism (Vimont *et al.*, 2003; Alexander *et al.*, 2010). These intra-seasonal mechanisms may have undergone a systematic change in the pre and post-shift years due to internal decadal variability that affects the strength of the low-level convergence feedback (Xiang *et al.*, 2013). Yu *et al.* (2012a) suggested that changes in the tropical atmospheric circulation (strengthening of the Hadley circulation and weakening of the Walker cell) could have played an active role in increasing the influence of the NPO in the post-shift years. The reported zonal shift in

the centers of action of the NPO (Yeh *et al.*, 2018) can contribute to the changing air-sea interactions and thus favouring CP-type ENSO events in the more recent decades. However, we would argue that shifts in southern pole of the NPO pattern could not develop independent of the tropical circulation changes and therefore likely reflect in parts the tropical circulation changes reported by Yu *et al.* (2012a).

Other researchers emphasize that the Pacific Meridional Mode (PMM) provides a link between atmospheric circulation anomalies with subtropical SST anomalies (Vimont *et al.*, 2003; Yeh *et al.*, 2015; Stuecker, 2018). Shin and An (2018) found that the PMM and NPO coupling strength experiences interdecadal changes that subsequently affect their ability to induce ENSO-like SST anomalies. The tendency has been an increasing coupling strength in recent decades. This would be consistent with the observed trends towards more CP ENSO events than EP after 1990. Further, it has been suggested that the position of the mid-latitude jet is important for PMM-NPO coupling (Johnson, 2013; Yu *et al.*, 2015; Alizadeh-Choobari, 2017). Stuecker (2018) points out that CP SST anomalies produce itself an extratropical atmospheric anomaly pattern that essentially constitutes a two-way coupling between tropics and extratropics, albeit involving different time scales.

However, mixed results have been reported with regard to the structure of the teleconnection pattern emerging from CP-type SST anomalies. Studies based on observations suggested that CP SST anomalies preferably induce NPO-like anomalies (Di Lorenzo *et al.*, 2010; Furtado *et al.*, 2012), whereas modelling studies (Geisler *et al.*, 1985; Stuecker, 2018) have found a preferred PNA-type response in the extratropical atmosphere. This translates into uncertainty regarding the response of the mid-latitude jet since PNA and NPO variability are linked with the strength/zonal extension and latitudinal position of the jet (Linkin and Nigam, 2008).

The complexity of the tropical-extratropical interactions and timescale dependency of the ocean-atmosphere feedbacks (Di Lorenzo *et al.*, 2010; Furtado *et al.*, 2012; Stuecker, 2018) impose a challenging task for finding a conclusive explanation for the observed changes in the correlations that were reported in this study. In addition, the lead-lag correlations between NPO and tropical SST response are sensitive to the definition of the NPO (Chen and Wu, 2018). This implies that the statistical analysis of the lag-0 correlations between NPO, ENSO and PNA can only be regarded as one piece of evidence that changes in the tropical-subtropical (and extratropical) interactions took place in the North Pacific during recent decades.

To summarize the discussion of the physical mechanisms, the shift towards CP ENSO events coincides

temporally with the decadal-scale shift in the PDO and NPO phases, North Pacific jet changes, and changes in the tropical-to-extratropical teleconnection pattern. The imprint of these climatic anomalies is seen in the statistical relationships between synoptic weather activity over the Hawaiian Islands and ENSO, NPO and PNA. The presented results and the discussion concentrated on the relationship between NPO, PNA, PDO and ENSO. It should be noted the North Pacific Gyre Oscillation (NPGO; Di Lorenzo *et al.*, 2008) is the oceanic counterpart to the NPO mode and should be included in upcoming studies regarding oceanic influences on regional climate variability and synoptic activity over the Central North Pacific. NPGO and NPO together appear to be equally important for understanding the decadal-to multidecadal variability in the North Pacific sector (Furtado *et al.*, 2012; Yu and Zou, 2013).

Although low statistical significance was found in the presented data analysis, this study re-iterates the importance of the mid-latitude jet structure in understanding long-term changes in the tropical-extratropical climate interactions. The Hawaiian Islands are located in a unique region in the central subtropical Pacific relative to the position of the mid-latitude jet exit region, which makes it susceptible to interdecadal changes in the climate system. In particular, Hawai'i's wet-season rainfall variability might be more sensitive than, for example, downstream regions in the western parts of North America due to its position relative to the mid-latitude zonal jet exit region (although Sung *et al.* (2019) have shown that temperature response patterns depend strongly on the strength and position of the NPO).

## 5 | SUMMARY AND CONCLUSION

This study presented a statistical analysis of various indices measuring large-scale climate variability and synoptic activity in the central subtropical Pacific over the Hawaiian Island region. The correlation analysis indicated that North Pacific climate variability on decadal to multidecadal timescales modulates the strength of the correlation between large-scale climate modes and synoptic activity over the Hawaiian Islands. In the early years between 1980 and 1994, ENSO variability had a stronger influence on the Hawaiian climate than in the later years 1995–2014 (1995–2012, depending on the analysed data sets). The apparent shift in the correlations coincides with transition of the PDO from a positive phase into predominantly neutral to negative PDO index values. At the same time, the NPO became more influential and contributed to the year to year rainfall variability. The reason

for the change in the correlations can be in parts explained by a systematic shift in the North Pacific jet position. A strong eastward elongated westerly wind jet was present in the earlier years while the jet was retracted more to the west since the mid-1990s.

This observation-based study suggests that these changes are part of the natural climate variability in connection with changes in PDO, NPO and ENSO modes. Previous modelling studies qualitatively support our result that decadal/multidecadal Pacific SST anomalies associated with the PDO can affect ENSO teleconnection pattern. However, the PDO phase change during the 1990s coincides with decadal-scale variations in the North Pacific ocean-atmosphere system related to the NPO (and NPGO). This mode is equally important for understanding the tropical to extratropical climate variability in the central North Pacific. Regional climate studies for the subtropical Hawaiian Islands should include the PDO/PNA as well as NPGO/NPO in the analysis of decadal to multidecadal variability.

The results from this analysis are a reminder that paleoclimatic interpretations based on univariate proxy information, whether from Hawai'i or other regions, have to be carefully evaluated. Biases can be introduced for example in the reconstructed signal amplitude of ENSO variability, or in the reconstruction of mean changes in the equatorial Pacific SST during the Holocene (Uchikawa *et al.*, 2010). It remains to be tested to what extent multivariate proxy data (for example, such as the recent SLP reconstructions [Diaz *et al.*, 2016]) can resolve such biases.

We further conclude that changes in teleconnection pattern due to internal modes of climate variability impose a source of uncertainty in applications of regional climate downscaling for future climate change studies. For example, shifting the observational data period that is used in the development of the statistical downscaling models (Elison Timm *et al.*, 2015) or in pseudo-global warming experiments (Zhang *et al.*, 2016) could significantly affect the magnitude of future rainfall change projections.

## ACKNOWLEDGEMENTS


The authors thank the editor and two anonymous reviewers for their constructive feedback. Their criticism that helped us to improve the manuscript. Abby Frazier, Thomas Giambelluca, Ryan Longman, Charly Massa, and Henry Diaz are acknowledged for the stimulating scientific discussions. They helped us with the interpretation of the synoptic variability and rainfall anomalies over the Hawaiian Islands. We like to thank Andrew Winters sharing his NPJ PC time series with us.

## CONFLICT OF INTEREST

The authors declare that they have no conflict of interest.

## ORCID

Oliver Elison Timm  <https://orcid.org/0000-0001-8871-0602>

David W. Beilman  <https://orcid.org/0000-0002-2625-6747>

## REFERENCES

- Alexander, M.A., Vimont, D.J., Chang, P. and Scott, J.D. (2010) The impact of extratropical atmospheric variability on ENSO: testing the seasonal footprinting mechanism using coupled model experiments. *Journal of Climate*, 23(11), 2885–2901. <https://doi.org/10.1175/2010JCLI3205.1>.
- Alizadeh-Choobari, O. (2017) Contrasting global teleconnection features of the eastern Pacific and Central Pacific El Niño events. *Dynamics of Atmospheres and Oceans*, 80, 139–154. <https://doi.org/10.1016/j.dynatmoce.2017.10.004>.
- Ashok, K., Behera, S.K., Rao, S.A., Weng, H. and Yamagata, T. (2007) El Niño Modoki and its possible teleconnection. *Journal of Geophysical Research, Oceans*, 112(11), 1–27. <https://doi.org/10.1029/2006JC003798>.
- Berry, G., Reeder, M.J. and Jakob, C. (2011) A global climatology of atmospheric fronts. *Geophysical Research Letters*, 38(4), 1–5. <https://doi.org/10.1029/2010GL046451>.
- Canty, A. and Ripley, B. D. (2017) ‘Boot: bootstrap R (S-Plus) functions’. Available at: <https://cran.r-project.org/web/packages/boot/index.html>.
- Cao, G., Giambelluca, T.W., Stevens, D.E. and Schroeder, T.A. (2007) Inversion variability in the Hawaiian trade wind regime. *Journal of Climate*, 20(7), 1145–1160. <https://doi.org/10.1175/JCLI4033.1>.
- Capotondi, A. and Sardeshmukh, P.D. (2017) Is El Niño really changing? *Geophysical Research Letters*, 44(16), 8548–8556. <https://doi.org/10.1002/2017GL074515>.
- Capotondi, A., Wittenberg, A.T., Newman, M., di Lorenzo, E., Yu, J.Y., Braconnot, P., Cole, J., Dewitte, B., Giese, B., Guilyardi, E., Jin, F.F., Karnauskas, K., Kirtman, B., Lee, T., Schneider, N., Xue, Y. and Yeh, S.W. (2015) Understanding ENSO diversity. *Bulletin of the American Meteorological Society*, 96(6), 921–938. <https://doi.org/10.1175/BAMS-D-13-00117.1>.
- Caruso, S.J. and Businger, S. (2006) Subtropical cyclogenesis over the central North Pacific\*. *Weather and Forecasting*, 21(2), 193–205. <https://doi.org/10.1175/WAF914.1>.
- Chen, S. and Wu, R. (2018) Impacts of winter NPO on subsequent winter ENSO: sensitivity to the definition of NPO index. *Climate Dynamics*, 50(1–2), 375–389. <https://doi.org/10.1007/s00382-017-3615-z>.
- Chen, Y.R. and Chu, P. (2014) Trends in precipitation extremes and return levels in the Hawaiian islands under a changing climate. *International Journal of Climatology*, 34(15), 3913–3925. <https://doi.org/10.1002/joc.3950>.
- Chu, P.-S. (1995) Hawaii rainfall anomalies and El Niño. *Journal of Climate*, 8(6), 1697–1703. [https://doi.org/10.1175/1520-0442\(1995\)008<1697:HRAAEN>2.0.CO;2](https://doi.org/10.1175/1520-0442(1995)008<1697:HRAAEN>2.0.CO;2).
- Chu, P.-S. and Chen, H. (2005) Interannual and interdecadal rainfall variations in the Hawaiian islands\*. *Journal of Climate*, 18(22), 4796–4813. <https://doi.org/10.1175/JCLI3578.1>.
- Chu, P.S., Chen, Y.R. and Schroeder, T.A. (2010) Changes in precipitation extremes in the Hawaiian islands in a warming climate. *Journal of Climate*, 23(18), 4881–4900. <https://doi.org/10.1175/2010JCLI3484.1>.
- Davison, A. C. and Hinkley, D. V (1997) *Bootstrap Methods and their Applications*. Cambridge: Cambridge University Press. Available at: <http://statwww.epfl.ch/davison/BMA/>.
- Dee, D.P., Uppala, S.M., Simmons, A.J., Berrisford, P., Poli, P., Kobayashi, S., Andrae, U., Balmaseda, M.A., Balsamo, G., Bauer, P., Bechtold, P., Beljaars, A.C.M., van de Berg, L., Bidlot, J., Bormann, N., Delsol, C., Dragani, R., Fuentes, M., Geer, A.J., Haimberger, L., Healy, S.B., Hersbach, H., Hólm, E. V., Isaksen, I., Kållberg, P., Köhler, M., Matricardi, M., McNally, A.P., Monge-Sanz, B.M., Morcrette, J.J., Park, B.K., Peubey, C., de Rosnay, P., Tavolato, C., Thépaut, J.N. and Vitart, F. (2011) The ERA-interim reanalysis: configuration and performance of the data assimilation system. *Quarterly Journal of the Royal Meteorological Society*, 137(656), 553–597. <https://doi.org/10.1002/qj.828>.
- Di Lorenzo, E., et al. (2008) North Pacific gyre oscillation links ocean climate and ecosystem change. *Geophysical Research Letters*, 35(8), 2–7. <https://doi.org/10.1029/2007GL032838>.
- Di Lorenzo, E., et al. (2010) Central Pacific El Niño and decadal climate change in the North Pacific Ocean. *Nature Geoscience*, 3(11), 762–765. <https://doi.org/10.1038/ngeo984>.
- Diaz, H.F., Wahl, E.R., Zorita, E., Giambelluca, T.W. and Eischeid, J.K. (2016) A five-century reconstruction of Hawaiian islands winter rainfall. *Journal of Climate*, 29(15), 5661–5674. <https://doi.org/10.1175/JCLI-D-15-0815.1>.
- Dong, B. and Dai, A. (2015) The influence of the interdecadal Pacific oscillation on temperature and precipitation over the globe. *Climate Dynamics*, 45(9–10), 2667–2681. <https://doi.org/10.1007/s00382-015-2500-x>.
- Dong, B., Dai, A., Vuille, M. and Timm, O.E. (2018) Asymmetric modulation of ENSO teleconnections by the interdecadal Pacific oscillation. *Journal of Climate*, 31(18), 7337–7361. <https://doi.org/10.1175/JCLI-D-17-0663.1>.
- Elison Timm, O., Diaz, H.F., Giambelluca, T.W. and Takahashi, M. (2011) Projection of changes in the frequency of heavy rain events over Hawaii based on leading Pacific climate modes. *Journal of Geophysical Research*, 116(D4), D04109. <https://doi.org/10.1029/2010JD014923>.
- Elison Timm, O., Giambelluca, T.W. and Diaz, H.F. (2015) Statistical downscaling of rainfall changes in Hawai‘i based on the CMIP5 global model projections. *Journal of Geophysical Research – Atmospheres*, 120(1), 92–112. <https://doi.org/10.1002/2014JD022059>.
- Elison Timm, O., Takahashi, M., Giambelluca, T.W. and Diaz, H.F. (2013) On the relation between large-scale circulation pattern and heavy rain events over the Hawaiian islands: recent trends and future changes. *Journal of Geophysical Research-Atmospheres*, 118(10), 4129–4141. <https://doi.org/10.1002/jgrd.50314>.
- Frazier, A.G., Elison Timm, O., Giambelluca, T.W. and Diaz, H.F. (2018) The influence of ENSO, PDO and PNA on secular rainfall variations in Hawai‘i. *Climate Dynamics*, 51(5–6), 2127–2140. <https://doi.org/10.1007/s00382-017-4003-4>.
- Frazier, A.G. and Giambelluca, T.W. (2017) Spatial trend analysis of Hawaiian rainfall from 1920 to 2012. *International Journal of Climatology*, 37(5), 2522–2531. <https://doi.org/10.1002/joc.4862>.
- Frazier, A.G., Giambelluca, T.W., Diaz, H.F. and Needham, H.L. (2016) Comparison of geostatistical approaches to spatially interpolate month-year rainfall for the Hawaiian islands.

- International Journal of Climatology*, 36(3), 1459–1470. <https://doi.org/10.1002/joc.4437>.
- Furtado, J.C., di Lorenzo, E., Anderson, B.T. and Schneider, N. (2012) Linkages between the North Pacific oscillation and central tropical Pacific SSTs at low frequencies. *Climate Dynamics*, 39(12), 2833–2846. <https://doi.org/10.1007/s00382-011-1245-4>.
- Geisler, J.E., Blackmon, M.L., Bates, G.T. and Muñoz, S. (1985) Sensitivity of January climate response to the magnitude and position of equatorial Pacific Sea surface temperature anomalies. *Journal of the Atmospheric Sciences*, 42(10), 1037–1049. [https://doi.org/10.1175/1520-0469\(1985\)042<1037:SOJCRT>2.0.CO;2](https://doi.org/10.1175/1520-0469(1985)042<1037:SOJCRT>2.0.CO;2).
- Gershunov, A. and Barnett, T.P. (1998) Interdecadal modulation of ENSO teleconnections. *Bulletin of the American Meteorological Society*, 79(12), 2715–2725. [https://doi.org/10.1175/1520-0477\(1998\)079<2715:IMOET>2.0.CO;2](https://doi.org/10.1175/1520-0477(1998)079<2715:IMOET>2.0.CO;2).
- Guo, Y., Wen, Z. and Wu, R. (2016) Interdecadal change in the tropical Pacific precipitation anomaly pattern around the late 1990s during boreal spring. *Journal of Climate*, 29(16), 5979–5997. <https://doi.org/10.1175/JCLI-D-15-0462.1>.
- Hu, Z.-Z. and Huang, B. (2009) Interferential impact of ENSO and PDO on dry and wet conditions in the US great plains. *Journal of Climate*, 22(22), 6047–6065. <https://doi.org/10.1175/2009JCLI2798.1>.
- Johnson, N.C. (2013) How many ENSO flavors can we distinguish?\*. *Journal of Climate*, 26(13), 4816–4827. <https://doi.org/10.1175/JCLI-D-12-00649.1>.
- Kaiser, L.R. (2014) *Assessing the Impacts of Kona Lows on Rainfall: Variability and Spatial Patterns in the Hawaiian Islands*. Honolulu, HI: University of Hawaii at Manoa, 48 <https://scholar.space.manoa.hawaii.edu/handle/10125/101096>.
- Kao, H.Y. and Yu, J.Y. (2009) Contrasting eastern-Pacific and central-Pacific types of ENSO. *Journal of Climate*, 22(3), 615–632. <https://doi.org/10.1175/2008JCLI2309.1>.
- Kodama, K. and Barnes, G.M. (1997) Heavy rain events over the south-facing slopes of Hawaii: attendant conditions. *Weather and Forecasting*, 12, 347–367. [https://doi.org/10.1175/1520-0434\(1997\)012<0347:HREOTS>2.0.CO;2](https://doi.org/10.1175/1520-0434(1997)012<0347:HREOTS>2.0.CO;2).
- Kodama, K.R. and Businger, S. (1998) Weather and forecasting challenges in the Pacific region of the National weather service. *Weather and Forecasting*, 13(3), 523–546. [https://doi.org/10.1175/1520-0434\(1998\)013<0523:WAFKIT>2.0.CO;2](https://doi.org/10.1175/1520-0434(1998)013<0523:WAFKIT>2.0.CO;2).
- Kug, J.S., Jin, F.F. and An, S.I. (2009) Two types of El Niño events: cold tongue El Niño and warm pool El Niño. *Journal of Climate*, 22(6), 1499–1515. <https://doi.org/10.1175/2008JCLI2624.1>.
- Larkin, N.K. (2005) Global seasonal temperature and precipitation anomalies during El Niño autumn and winter. *Geophysical Research Letters*, 32(16), L16705. <https://doi.org/10.1029/2005GL022860>.
- Li, G., Chen, J., Wang, X., Tan, Y. and Jiang, X. (2017) Modulation of Pacific decadal oscillation on the relationship of El Niño with southern China rainfall during early boreal winter. *Atmospheric Science Letters*, 18(8), 336–341. <https://doi.org/10.1002/asl.761>.
- Liebmann, B., Marengo, J.A., Glick, J.D., Kousky, V.E., Wainer, I.C. and Massambani, O. (1998) A comparison of rainfall, outgoing longwave radiation, and divergence over the Amazon Basin. *Journal of Climate*, 11(11), 2898–2909. [https://doi.org/10.1175/1520-0442\(1998\)011<2898:ACOROL>2.0.CO;2](https://doi.org/10.1175/1520-0442(1998)011<2898:ACOROL>2.0.CO;2).
- Linkin, M. E. and Nigam, S. (2008) 'The North Pacific Oscillation-West Pacific teleconnection pattern: Mature-phase structure and winter impacts', *Journal of Climate*, 21(9), 1979–1997. <https://doi.org/10.1175/2007JCLI2048.1>.
- Longman, R.J., Diaz, H.F. and Giambelluca, T.W. (2015) Sustained increases in lower-tropospheric subsidence over the central tropical North Pacific drive a decline in high-elevation rainfall in Hawaii. *Journal of Climate*, 28(22), 8743–8759. <https://doi.org/10.1175/JCLI-D-15-0006.1>.
- Longman, R.J., O. Elison Timm, T.W. Giambelluca, and L. Kaiser, 2020. *A 20-year analysis of disturbance-driven rainfall on O'ahu, Hawai'i*, Mon. Wea. Rev., in review.
- McPhaden, M.J., Lee, T. and McClurg, D. (2011) El Niño and its relationship to changing background conditions in the tropical Pacific Ocean. *Geophysical Research Letters*, 38(15), 2–5. <https://doi.org/10.1029/2011GL048275>.
- Morrison, I. and Businger, S. (2001) Synoptic structure and evolution of a Kona low. *Weather and Forecasting*, 16(1), 81–98. [https://doi.org/10.1175/1520-0434\(2001\)016<0081:SSAEOA>2.0.CO;2](https://doi.org/10.1175/1520-0434(2001)016<0081:SSAEOA>2.0.CO;2).
- Nakuina, M.K. (2005) In: Mookini, E.T. and Nākoa, S. (Eds.) *The Wind Gourd of La'Amaomao*, Revised edition. Honolulu, HI: Kalamakū Press. [https://catalog.loc.gov/vwebv/search?searchArg=2005921737&searchCode=GKEY%5E\\*&searchType=1&limitTo=none&fromYear=&toYear=&limitTo=LOCA%3Dall&limitTo=PLAC%3Dall&limitTo=TYPE%3Dall&limitTo=LANG%3Dall&recCount=25](https://catalog.loc.gov/vwebv/search?searchArg=2005921737&searchCode=GKEY%5E*&searchType=1&limitTo=none&fromYear=&toYear=&limitTo=LOCA%3Dall&limitTo=PLAC%3Dall&limitTo=TYPE%3Dall&limitTo=LANG%3Dall&recCount=25).
- O'Connor, C.F., Chu, P.S., Hsu, P.C. and Kodama, K. (2015) Variability of Hawaiian winter rainfall during La Niña events since 1956. *Journal of Climate*, 28(19), 7809–7823. <https://doi.org/10.1175/JCLI-D-14-00638.1>.
- Otkin, J.A. and Martin, J.E. (2004a) A synoptic climatology of the subtropical Kona storm. *Monthly Weather Review*, 132(6), 1502–1517. [https://doi.org/10.1175/1520-0493\(2004\)132<1502:ascots>2.0.co;2](https://doi.org/10.1175/1520-0493(2004)132<1502:ascots>2.0.co;2).
- Otkin, J.A. and Martin, J.E. (2004b) The large-scale modulation of subtropical cyclogenesis in the central and eastern Pacific Ocean. *Monthly Weather Review*, 132(7), 1813–1828. [https://doi.org/10.1175/1520-0493\(2004\)132<1813:TLMOSC>2.0.CO;2](https://doi.org/10.1175/1520-0493(2004)132<1813:TLMOSC>2.0.CO;2).
- R Core Team. (2015) *R: A Language and Environment for Statistical Computing*. Vienna, Austria. Available at. <https://cran.r-project.org/doc/FAQ/R-FAQ.html#Citing-R>. <https://doi.org/10.1017/CBO9780511803642>
- Ren, H.L. and Jin, F.F. (2013) Recharge oscillator mechanisms in two types of ENSO. *Journal of Climate*, 26(17), 6506–6523. <https://doi.org/10.1175/JCLI-D-12-00601.1>.
- Rodionov, S. and Overland, J.E. (2005) Application of a sequential regime shift detection method to the Bering Sea ecosystem. *ICES Journal of Marine Science*, 62(3), 328–332. <https://doi.org/10.1016/j.icesjms.2005.01.013>.
- Rodionov, S.N. (2004) A sequential algorithm for testing climate regime shifts. *Geophysical Research Letters*, 31(9), 2–5. <https://doi.org/10.1029/2004GL019448>.
- Schulzweida, U. (2019) 'CDO User Guide'. doi: <https://doi.org/10.5281/zenodo.3539275>.
- Seager, R., Naik, N., Ting, M., Cane, M.A., Harnik, N. and Kushnir, Y. (2010) Adjustment of the atmospheric circulation to tropical Pacific sst anomalies: variability of transient eddy propagation in the pacific-North America sector. *Quarterly Journal of the Royal Meteorological Society*, 136(647), 277–296. <https://doi.org/10.1002/qj.588>.
- Shaw, T.A. and Pauluis, O. (2012) Tropical and subtropical meridional latent heat transports by disturbances to the zonal mean



- and their role in the general circulation. *Journal of the Atmospheric Sciences*, 69(6), 1872–1889. <https://doi.org/10.1175/JAS-D-11-0236.1>.
- Shin, S.-J. and An, S.-I. (2018) Interdecadal change in the relationship between the North Pacific oscillation and the Pacific meridional mode and its impact on ENSO. *Asia-Pacific Journal of Atmospheric Sciences*, 54(1), 63–76. <https://doi.org/10.1007/s13143-017-0060-1>.
- Simpson, R.H. (1952) Evolution of the Kona storm, a subtropical cyclone. *Journal of Meteorology*, 9(1), 24–35. [https://doi.org/10.1175/1520-0469\(1952\)009<0024:EOTKSA>2.0.CO;2](https://doi.org/10.1175/1520-0469(1952)009<0024:EOTKSA>2.0.CO;2).
- Stirnemann, L., Conversi, A. and Marini, S. (2019) Detection of regime shifts in the environment: testing “STARS” using synthetic and observed time series. *ICES Journal of Marine Science*, 76(7), 2286–2296. <https://doi.org/10.1093/icesjms/fsz148>.
- Stuecker, M.F. (2018) Revisiting the Pacific meridional mode. *Scientific Reports*, 8(1), 1–9. <https://doi.org/10.1038/s41598-018-21537-0>.
- Sung, M.K., Jang, H.Y., Kim, B.M., Yeh, S.W., Choi, Y.S. and Yoo, C. (2019) Tropical influence on the North Pacific oscillation drives winter extremes in North America. *Nature Climate Change*, 9(5), 413–418. <https://doi.org/10.1038/s41558-019-0461-5>.
- Tan, J., Jakob, C. and Lane, T.P. (2013) On the identification of the large-scale properties of tropical convection using cloud regimes. *Journal of Climate*, 26(17), 6591–6617. <https://doi.org/10.1175/JCLI-D-12-00624.1>.
- Uchikawa, J., et al. (2010) Geochemical and climate modeling evidence for Holocene aridification in Hawaii: dynamic response to a weakening equatorial cold tongue. *Quaternary Science Reviews*, 29(23–24), 3057–3066. <https://doi.org/10.1016/j.quascirev.2010.07.014>.
- Vimont, D.J., Wallace, J.M. and Battisti, D.S. (2003) The seasonal footprinting mechanism in the Pacific: implications for ENSO\*. *Journal of Climate*, 16(16), 2668–2675. [https://doi.org/10.1175/1520-0442\(2003\)016<2668:TSMIT>2.0.CO;2](https://doi.org/10.1175/1520-0442(2003)016<2668:TSMIT>2.0.CO;2).
- Walker, C.C. and Schneider, T. (2006) Eddy influences on Hadley circulations: simulations with an idealized GCM. *Journal of the Atmospheric Sciences*, 63(12), 3333–3350. <https://doi.org/10.1175/JAS3821.1>.
- Wen, C., Kumar, A. and Xue, Y. (2014) ‘Factors contributing to uncertainty in Pacific Decadal Oscillation index’, *Geophysical Research Letters*, 41(22), 7980–7986. doi: <https://doi.org/10.1002/2014GL061992>.
- Wilks, D.S. (2016) “The stippling shows statistically significant grid points”: how research results are routinely overstated and over-interpreted, and what to do about it. *Bulletin of the American Meteorological Society*, 97(12), 2263–2273. <https://doi.org/10.1175/BAMS-D-15-00267.1>.
- Winters, A.C., Keyser, D. and Bosart, L.F. (2019) The development of the North Pacific jet phase diagram as an objective tool to monitor the state and forecast skill of the upper-tropospheric flow pattern. *Weather and Forecasting*, 34(1), 199–219. <https://doi.org/10.1175/waf-d-18-0106.1>.
- Xiang, B., Wang, B. and Li, T. (2013) A new paradigm for the pre-dominance of standing central Pacific warming after the late 1990s. *Climate Dynamics*, 41(2), 327–340. <https://doi.org/10.1007/s00382-012-1427-8>.
- Yeh, S.W., Wang, X., Wang, C. and Dewitte, B. (2015) On the relationship between the North Pacific climate variability and the Central Pacific El Niño. *Journal of Climate*, 28(2), 663–677. <https://doi.org/10.1175/JCLI-D-14-00137.1>.
- Yeh, S.W., Yi, D.W., Sung, M.K. and Kim, Y.H. (2018) An eastward shift of the North Pacific oscillation after the mid-1990s and its relationship with ENSO. *Geophysical Research Letters*, 45(13), 6654–6660. <https://doi.org/10.1029/2018GL078671>.
- Yu, J.-Y. and Kim, S.T. (2011) Relationships between Extratropical Sea level pressure variations and the Central Pacific and eastern Pacific types of ENSO. *Journal of Climate*, 24(3), 708–720. <https://doi.org/10.1175/2010JCLI3688.1>.
- Yu, J.Y., Lu, M.M. and Kim, S.T. (2012a) A change in the relationship between tropical Central Pacific SST variability and the extratropical atmosphere around 1990. *Environmental Research Letters*, 7(3), 034025. <https://iopscience.iop.org/article/10.1088/1748-9326/7/3/034025>.
- Yu, J.-Y., Paek, H., Saltzman, E.S. and Lee, T. (2015) The early 1990s change in ENSO–PSA–SAM relationships and its impact on southern hemisphere climate. *Journal of Climate*, 28(23), 9393–9408. <https://doi.org/10.1175/JCLI-D-15-0335.1>.
- Yu, J.-Y. and Zou, Y. (2013) The enhanced drying effect of Central-Pacific El Niño on US winter. *Environmental Research Letters*, 8(1), 014019. <https://doi.org/10.1088/1748-9326/8/1/014019>.
- Yu, J.Y., Zou, Y., Kim, S.T. and Lee, T. (2012b) The changing impact of El Niño on US winter temperatures. *Geophysical Research Letters*, 39(15), L15702. <https://agupubs.onlinelibrary.wiley.com/doi/full/10.1029/2012GL052483>.
- Zhang, C., Wang, Y., Hamilton, K. and Lauer, A. (2016) Dynamical downscaling of the climate for the Hawaiian islands. Part II: projection for the late twenty-first century. *Journal of Climate*, 29(23), 8333–8354. <https://doi.org/10.1175/JCLI-D-16-0038.1>.

## SUPPORTING INFORMATION

Additional supporting information may be found online in the Supporting Information section at the end of this article.

**How to cite this article:** Elison Timm O, Li S, Liu J, Beilman DW. On the changing relationship between North Pacific climate variability and synoptic activity over the Hawaiian Islands. *Int J Climatol*. 2021;41 (Suppl. 1):E1566–E1582. <https://doi.org/10.1002/joc.6789>